NATIONAL ADVISORY COMMITTEE FOR AERONAUTICS

TECHNICAL NOTE 2992

APPLICATION OF A CHARACTERISTIC BLADE-TO-BLADE SOLUTION TO FLOW IN A SUPERSONIC ROTOR WITH VARYING STREAM-FILAMENT THICKNESS

By Eleanor L. Costilow

Lewis Flight Propulsion Laboratory
Cleveland, Ohio

Washington
August 1953

NATIONAL ADVISORY COMMITTEE FOR AERONAUTICS

TECHNICAL NOTE 2992

APPLICATION OF A CHARACTERISTIC BLADE-TO-BLADE SOLUTION TO FLOW IN A SUPERSONIC ROTOR WITH VARYING STREAM-FILAMENT THICKNESS

By Eleanor L. Costilow

ERRATA

NACA TN 2992

APPLICATION OF A CHARACTERISTIC BLADE-TO-BLADE SOLUTION TO FLOW IN A SUPERSONIC ROTOR WITH VARYING STREAM-FILAMENT THICKNESS
By Eleanor L. Costilow

August 1953

Page 7, (eq. (11)): The right sides of the equations for coefficients L and N should be preceded by minus signs.

~~blade cannot, in general, be considered on an ordinary two-~~ dimensional basis. Annular area reductions of the order of two to one, or of higher orders, may occur, making it necessary to include the effect of radial variation in stream-filament height and curvature in the meridional plane in a blade-to-blade solution. It appears feasible to obtain a more complete analysis of the impeller flow by a reiterative calculation procedure along two different types of relative flow surfaces. A description of the two flow surfaces, called S_1 (a blade-to-blade type of surface) and S_2 (a meridional type of surface), and the equations for calculating the supersonic flow on both kinds of surfaces can be found in reference 1.

As a first approximation to the complete flow description, the stream-filament-thickness variation to be used in the calculation of the S_1 surface of revolution may be determined by an axisymmetric solution in the meridional plane. A method for such an axisymmetric solution is described and worked out in detail with examples in reference 2. A solution of this type gives the flow variations along the blade span; however, the blade-to-blade solution must be approximated from the axisymmetric supersonic solution, blade circulation, and continuity. A total of 160 hours of hand computing is required for 100 grid points in the meridional plane. A solution of the type of reference 2 is necessary to give the stream-sheet thickness and curvature for the blade-to-blade (S_1 surface) solution considered in this report. The equations for the solution of the S_1 surface of revolution are presented in reference 3.

The purpose of the subject report is to continue the work of reference 3 by applying the method to a specific problem in order that the practicability of the method and the time involved in computing a solution may be determined. The calculation procedure used in the application of the method is outlined in detail.

Once this blade-to-blade solution is obtained, a finer approximation to the flow may be obtained by computing the flow on several S_2 surfaces and by then repeating the computation on S_1 surfaces which are no longer surfaces of revolution as described in reference 1.

The tip stream filament of a constant-tip-diameter supersonic impeller was chosen for illustrating the numerical technique inasmuch as it was originally proposed to separate the stream-filament-thickness effect from the stream-curvature effect. For S_1 surfaces of revolution other than the tip, the calculation time required will be increased slightly over the 1/2 hour per grid point estimated here, since, for this case, it is necessary to include stream-filament slope terms. It is felt that the additional calculating time required will not be excessive.

For completeness, the equations given in reference 3 have been derived from a different approach for a fluid with negligible entropy change and a constant-modified-relative stagnation enthalpy. The equations are given in finite difference form for the general surface of revolution, and the computing procedure is detailed for the case where the surface-of-revolution curvature is neglected.

SYMBOLS

The following symbols are used in this report:

A	area normal to flow
A_{cr}	critical area (at $M = 1$)
a	local speed of sound
h	static enthalpy
J,L,N	coefficients in characteristic equations
K	constant
ζ, φ	orthogonal coordinates on mean surface of revolution
M	local Mach number
$\bar{n}$	unit vector normal to surface of revolution
P	total pressure
p	static pressure
r	radial distance from axis of machine (fig. 1)
T	thickness parameter
V	absolute velocity
W	relative velocity
z	distance measured along axis of machine (fig. 1)
β	relative flow angle, $\tan^{-1} W_\varphi/W_\zeta$
γ	ratio of specific heats, 1.4
δ	flow angle correction term, equation (B2)
ϵ	Prandtl angle correction term, equation (B1)
η	first characteristic family
λ	slope of characteristic curve on mean surface of revolution

μ Mach angle, $\sin^{-1} 1/M$

ν Prandtl-Meyer angle

ξ second characteristic family

ρ mass density

σ slope of mean surface of revolution in meridional plane, $\tan^{-1} W_r/W_z$

τ normal thickness of stream filament of revolution

ψ stream function

ω angular velocity of blade

Subscripts:

a stagnation conditions

i inlet

l, φ meridional and circumferential components

r,z components in r- and z-directions, respectively

t tip

1,2,3 points of characteristic net

o two-dimensional solution

+,- characteristic slope of 1st and 2nd characteristics

Superscripts:

$*$ dimensionless values, lengths are normalized by the tip radius and velocity by the stagnation speed of sound

$\rightarrow$ vector velocity

DEVELOPMENT OF GENERAL EQUATIONS

The flow equations for supersonic flow on a general surface of revolution with variable stream-filament thickness $\tau = \tau(l)$ (see fig. 1)

can be developed from the equation of continuity and the absolute vorticity normal to the surface of revolution.

For steady flow the continuity equation becomes:

$$\frac{\partial(\tau\rho W_\zeta r)}{\partial \zeta} + \frac{\partial(\tau\rho W_\varphi)}{\partial \varphi} = 0 \tag{1}$$

If the flow is isentropic such that

$$\rho = Kh^{\frac{1}{\gamma-1}}$$

the continuity equation may be written as:

$$\frac{\partial\left(\tau W_\zeta r h^{\frac{1}{\gamma-1}}\right)}{\partial \zeta} + \frac{\partial\left(\tau W_\varphi h^{\frac{1}{\gamma-1}}\right)}{\partial \varphi} = 0 \tag{2}$$

Assuming that the absolute vorticity of the flow field is zero, then

$$\nabla \times \bar{V} \equiv \nabla \times (\bar{W} + \bar{\omega} \times \bar{r}) \equiv \nabla \times \bar{W} + 2\bar{\omega} = 0 \tag{3}$$

The equation for the vorticity that involves the velocities W_ζ and W_φ on the surface of revolution is needed to combine with the continuity equation. The vorticity normal to the surface of revolution is a function of these surface velocities. The vorticity normal to the surface of revolution in vector notation is

$$\bar{n} \cdot (\nabla \times \bar{W} + 2\bar{\omega}) = 0$$

This relation, when expended in terms of W_φ and W_ζ using the method of reference 4 (p. 210, eq. 9), is

$$\frac{1}{r}\frac{\partial W_\zeta}{\partial \varphi} - \frac{\partial W_\varphi}{\partial \zeta} - \left(\frac{W_\varphi}{r} + 2\omega\right) \sin \sigma = 0 \tag{4}$$

For convenience it is desirable to express the continuity and vorticity equations in terms of the relative velocity W and the flow angle β:

$$W_\zeta = W \cos \beta$$

$$W_\varphi = W \sin \beta$$

Differentiating equations (2) and (4) and substituting the relations for the velocity components, the following equations result where $h = \frac{a^2}{\gamma-1}$:

$$\frac{\cot^2\mu}{W}\frac{\partial W}{\partial l} + \frac{\tan\beta\cot^2\mu}{W}\frac{\partial W}{r\partial\varphi} + \tan\beta\frac{\partial\beta}{\partial l} - \frac{\partial\beta}{r\partial\varphi} - \left(\frac{\omega^2 r\sin\sigma}{a^2} + \frac{\sin\sigma}{r} + \frac{\partial \ln\tau}{\partial l}\right) = 0 \tag{5}$$

and

$$\frac{\tan\beta}{W}\frac{\partial W}{\partial l} - \frac{1}{W}\frac{\partial W}{r\partial\varphi} + \frac{\partial\beta}{\partial l} + \tan\beta\frac{\partial\beta}{r\partial\varphi} + \frac{1}{W\cos\beta}\left(\frac{W\sin\beta}{r} + 2\omega\right)\sin\sigma = 0 \tag{6}$$

Applying the method of characteristics to equations (5) and (6) according to reference 5 (pp. 38-45), two families of characteristic lines are obtained. The two types of characteristic lines will be denoted by the characteristic parameters η and ξ, where η varies along a ξ-constant-characteristic line and ξ varies along an η-constant-characteristic line. The characteristic equations become:

$$\frac{1}{W\tan\mu}\frac{\partial W}{\partial\xi} - \frac{\partial\beta}{\partial\xi} - \tan\mu\left[\frac{\omega^2 r\sin\sigma}{a^2} + \frac{\partial \ln\tau}{\partial l} + \frac{\lambda_-\sin\sigma\cos\beta}{r(\lambda_-\cos\beta-\sin\beta)} + \frac{1}{J}\frac{N\cos\beta - L\sin\beta}{(\lambda_-\cos\beta-\sin\beta)}\right]\frac{\partial l}{\partial\xi} = 0 \tag{7}$$

where the slope of the η-constant-characteristic line is

$$\lambda_+ = \frac{r\,d\varphi}{dl} = \tan(\beta+\mu) \tag{8}$$

Similarly, along a ξ-constant-characteristic line:

$$\frac{1}{W\tan\mu}\frac{\partial W}{\partial\eta} + \frac{\partial\beta}{\partial\eta} - \tan\mu\left[\frac{\omega^2 r\sin\sigma}{a^2} + \frac{\partial \ln\tau}{\partial l} + \frac{\lambda_+\sin\sigma\cos\beta}{r(\lambda_+\cos\beta-\sin\beta)} + \frac{1}{J}\frac{N\cos\beta - L\sin\beta}{(\lambda_+\cos\beta-\sin\beta)}\right]\frac{\partial l}{\partial\eta} = 0 \tag{9}$$

and the ξ-constant-characteristic line slope is

$$\lambda_{-} = \frac{r\,d\varphi}{dl} = \tan(\beta - \mu) \tag{10}$$

These characteristic lines are shown in figure 2.

The coefficients J, L, and N on characteristic equations (7) and (9) are:

$$\left.\begin{aligned} J &= \left(1 - \frac{\cos^2\beta}{\sin^2\mu}\right) \\ L &= \frac{1}{a^2}\left[\left(\omega^2 r + \frac{W^2\cos^2\beta}{r}\right)\sin\sigma + a^2\frac{\partial \ln \tau}{\partial l}\right] \\ N &= \left(1 - \frac{1}{\sin^2\mu}\right)\left[\left(\frac{W\sin\beta}{r} + 2\omega\right)\frac{\sin\sigma}{W\cos\beta}\right] \end{aligned}\right\} \tag{11}$$

Characteristic equations (7) and (9) are the same as equations (12a) and (12b) of reference 3 for a flow with uniform I and negligible entropy change, where I is the modified-relative stagnation enthalpy defined by

$$I = h + \frac{1}{2}W^2 - \frac{1}{2}\omega^2 r^2$$

A solution of the flow field is obtained by replacing the characteristic differential equations with a series of difference equations which are solved in a step-by-step procedure. Assume two characteristics emanating from points 1 and 2 and intersecting at point 3 as shown in figure 2 where the flow properties are known, one of them, η, with a slope equal to $\tan(\beta+\mu)_1$ and the other, ξ, having a slope $\tan(\beta-\mu)_2$. The coordinates l_3, φ_3 defining point 3 are determined from equations (8) and (10). Thus

$$\left.\begin{aligned} r_1(\varphi_3-\varphi_1) &= \lambda_{+1}(l_3-l_1) \quad (\eta \text{ constant}) \\ r_2(\varphi_3-\varphi_2) &= \lambda_{-2}(l_3-l_2) \quad (\xi \text{ constant}) \end{aligned}\right\} \tag{12}$$

After point 3 is established from equations (12), W_3 and β_3 are determined from the simultaneous solution of the characteristic equations. In finite difference form, equation (7) along η and equation (9) along ξ are

$$\frac{1}{W_1 \tan \mu_1}(W_3-W_1) - (\beta_3-\beta_1) - \tan \mu_1 \left[\frac{\omega^2 r \sin \sigma}{a^2} + \frac{\partial \ln \tau}{\partial l} + \frac{\lambda_- \sin \sigma \cos \beta}{r(\lambda_- \cos \beta - \sin \beta)} + \frac{1}{J}\frac{N \cos \beta - L \sin \beta}{(\lambda_- \cos \beta - \sin \beta)}\right]_1 (l_3-l_1) = 0 \quad (\eta \text{ constant}) \tag{13}$$

$$\frac{1}{W_2 \tan \mu_2}(W_3-W_2) + (\beta_3-\beta_2) - \tan \mu_2 \left[\frac{\omega^2 r \sin \sigma}{a^2} + \frac{\partial \ln \tau}{\partial l} + \frac{\lambda_+ \sin \sigma \cos \beta}{r(\lambda_+ \cos \beta - \sin \beta)} + \frac{1}{J}\frac{N \cos \beta - L \sin \beta}{(\lambda_+ \cos \beta - \sin \beta)}\right]_2 (l_3-l_2) = 0 \quad (\xi \text{ constant}) \tag{14}$$

For the case where a characteristic intersects a boundary rather than another characteristic as shown in figure 2, only one characteristic equation is needed, because either W_3 or β_3 will be known at the intersection point. In the case of an inverse problem either the velocity or blade turning is specified on the blade surface, and in a direct problem the blade angle is known at the point of intersection.

The computational procedure to determine the properties and location of point 3 involves an iteration process. The initial solution at point 3 is determined with the coefficients of $(\varphi_3-\varphi_{1,2})$, $(l_3-l_{1,2})$, $(W_3-W_{1,2})$, and $(\beta_3-\beta_{1,2})$ based on the values at points 1 and 2. In succeeding approximations to the values at 3, the coefficients based on the preceding values at point 3 are determined and averaged with the coefficients at 1 and 2, so that after the first approximation to 3, all coefficients subscripted 1 and 2 are coefficients averaged between 1 and 3 and between 2 and 3. The calculation procedure for the values at 3 is repeated until the solution at point 3 converges within the accuracy desired and the process is carried downstream step by step.

CHARACTERISTIC EQUATIONS FOR TIP STREAM FILAMENT

In this report the general characteristics method described has been simplified for application to the tip section of a constant-tip-diameter supersonic compressor. The numerical analysis takes into account a variable stream-filament thickness but ignores the effect of stream-filament curvature in the meridional plane since this effect will be small at the specified tip section. In the case of a tip stream filament the following conditions hold:

$$\left.\begin{aligned} l &= z \\ r &= r_t = \text{constant} \\ \tau &= \tau(z) \\ \sigma &= 0^\circ \end{aligned}\right\} \tag{15}$$

When these conditions are applied to characteristic equations (7) and (9), the characteristic equations for the tip section become:

$$\frac{1}{W \tan \mu}\frac{\partial W}{\partial \xi} - \frac{\partial \beta}{\partial \xi} + \frac{\cot \beta \tan \mu}{\tan \mu - \cot \beta}\frac{\partial \ln \tau}{\partial \xi} = 0 \tag{16}$$

$$\frac{1}{W \tan \mu}\frac{\partial W}{\partial \eta} + \frac{\partial \beta}{\partial \eta} - \frac{\cot \beta \tan \mu}{\tan \mu + \cot \beta}\frac{\partial \ln \tau}{\partial \eta} = 0 \tag{17}$$

and from equations (8) and (10) their corresponding slope equations become:

$$\left.\begin{aligned} r_t(\varphi_3 - \varphi_1) &= \lambda_{+1}(z_3 - z_1) \quad (\eta \text{ constant}) \\ r_t(\varphi_3 - \varphi_2) &= \lambda_{-2}(z_3 - z_2) \quad (\xi \text{ constant}) \end{aligned}\right\} \tag{18}$$

If it is noted that the first term in equations (16) and (17) is the Prandtl-Meyer angle $d\nu$, the characteristic equations become the usual plane-flow characteristic equations (two-dimensional solution) plus a correction term for stream-filament thickness as seen from the following equations:

$$\frac{\partial \nu}{\partial \xi} - \frac{\partial \beta}{\partial \xi} + \frac{\cot \beta \tan \mu}{\tan \mu - \cot \beta}\frac{\partial \ln \tau}{\partial \xi} = 0 \tag{19}$$

$$\frac{\partial \nu}{\partial \eta} + \frac{\partial \beta}{\partial \eta} - \frac{\cot \beta \tan \mu}{\tan \mu + \cot \beta}\frac{\partial \ln \tau}{\partial \eta} = 0 \tag{20}$$

The plane-flow characteristic equations are simply

$$\frac{\partial \nu}{\partial \xi} - \frac{\partial \beta}{\partial \xi} = 0 \tag{21}$$

$$\frac{\partial \nu}{\partial \eta} + \frac{\partial \beta}{\partial \eta} = 0 \tag{22}$$

The analysis of the flow at the impeller tip was carried out using equations (19) and (20) together with the Ames tables (ref. 6).

ILLUSTRATIVE EXAMPLE

The characteristics method outlined in the preceding sections for solving the supersonic flow equations has been applied at the tip of a constant-tip-diameter supersonic impeller to determine the blade-to-blade flow properties. The blade shape at the tip is shown in figure 3. An estimated boundary-layer-thickness correction has been added to the blade profile varying linearly along the axial blade length from zero at the leading edge to 10 percent of the pitch distance at the exit. The actual profile is shown by the dotted line in figure 3. The stream-filament-thickness variation from inlet to exit is assumed to be the result of a solution as described in reference 2. This variation at the tip section is shown in figure 4, where it is noted that the thickness is reduced at the exit to 40 percent of the value at the inlet. In the example, this is the axial-stream-filament-thickness variation that is applied at the constant tip diameter (thickness remains constant tangentially); hence the stream-sheet curvature in the meridional plane was neglected. The quantities known at the leading edge were inlet angle β_1, -67.4°; inlet-flow deflection angle, 7°; suction-surface direction, -66.4°; inlet-Mach number M_1, 1.6563; inlet-stream-filament thickness T_1^*, 0.05; relative velocity W_1^*, 1.3308; pitch distance, 0.2167; and the axial-chord length, 0.625. Dimensionless quantities are denoted with an asterisk.

Special procedures not discussed previously were required in some phases of the numerical analysis because of the nature of the inlet conditions prescribed in the example and because of the leading-edge shock wave interaction with the characteristic lines. These phases of the calculations and the determination of the characteristic blade-to-blade solution will be discussed in the following sections.

Entrance region. - The solution of the flow equations by the method of characteristics assumes that the boundary conditions are known on an initial curve, in this case an inlet line, along which a series of points, such as 1 and 2 in figure 2, are selected from which to initiate the characteristics solution. In establishing this line, it is necessary first to investigate the properties in the inlet region of those characteristic curves which are known as expansion waves. In accordance with the coordinate system selected for this example, these curves are characteristic lines of constant ξ where λ_- is tan $(\beta-\mu)$. When the absolute value of the wave angle, $\beta-\mu$, is less than 90° so that the expansion waves from the leading edge are contained within the blade passage as shown by the dashed line in figure 5, the inlet conditions as prescribed prevail up to the blade leading edge. For such a case the characteristic solution is started by selecting a series of grid points along AB where the flow is known and applying the iteration process described earlier at points 1 and 2 for the solution at 3. The procedure is possible since, in addition to the initial conditions along the characteristic line, the flow direction on the two blade surfaces is known.

However, with inlet conditions of the magnitude selected for this example, it was found that the absolute value of the wave angle, $\beta-\mu$, at the leading edge was greater than 90° and the waves fell outside the blade passages. This type of wave system and the one described previously are characterized by the magnitude of the axial component of velocity. If the axial velocity component is supersonic, the waves will be contained within the blade passage, and if the axial component is subsonic, the waves fall upstream of the blade passage. For the latter condition where the flow upstream of each blade is influenced by the waves issuing from the neighboring blade, the usual prescription of uniform-flow conditions at the entrance to the blade passage can no longer be made and it becomes necessary to study the flow conditions in this region further.

In order to establish uniform-flow conditions at infinity upstream of the blade row for steady-state flow, it is necessary that no disturbance exist at infinity. Any wave system that is present in front of the blades must originate from the blades themselves in such a manner that the expansion waves produced are cancelled by the formation of equal compression waves. Since only one family of waves, ξ-constant characteristic family, extends upstream, a simple wave system will satisfy uniform-flow conditions at infinity.

For plane flow, the condition for a simple wave is merely $\nu = \nu(\xi)$, $\beta = \beta(\xi)$, which satisfies equation (22) and equation (21) with the solution $\nu-\beta$ equal to a constant. This method cannot be used with equations (19) and (20) because $\nu = \nu(\xi)$, $\beta = \beta(\xi)$ gives with equation (20) that $\partial\tau/\partial\eta = 0$, which is not satisfied. The characteristic equations (19) and (20) become somewhat simpler to study in terms of $W \sin\beta$ and a parameter

$$T = \tau h^{\frac{1}{\gamma-1}} W \cos\beta$$

When these variables are introduced, equations (19) and (20) become

$$\frac{1}{W \cos\beta \tan\mu}\frac{\partial(W \sin\beta)}{\partial\xi} + \frac{\partial(\ln T)}{\partial\xi} = 0 \tag{23}$$

$$\frac{1}{W \cos\beta \tan\mu}\frac{\partial(W \sin\beta)}{\partial\eta} - \frac{\partial(\ln T)}{\partial\eta} = 0 \tag{24}$$

In this case the condition $W \sin\beta = Y(\xi)$, $T = T(\xi)$ does not violate equation (24) but satisfies it identically; however, equation (23) is not satisfied in general because $1/W \cos\beta \tan\mu$ is a function of Y, T, and τ, and τ is a function of ξ and η. Differentiation of equation (23) with $\eta(Y = Y(\xi), T = T(\xi))$, gives the result

$$\frac{\partial Y}{\partial \xi}\frac{\partial}{\partial \tau}\left(\frac{1}{W \cos \beta \tan \mu}\right)\frac{\partial \tau}{\partial \eta} = 0$$

Thus there is the solution Y equal a constant, and hence from equation (23) T is also a constant.

For the example considered in this report, these conditions were not used and the actual flow was approximated by setting $Y = Y(\xi)$, $T = T(\xi)$ and integrating equation (19). It is estimated that the maximum error involved in ν-β is less than 0.07° when the approximate value of the coefficient of $d(\ln \tau)$ is used in equation (19). Equation (20) is satisfied exactly. The result of the integration is that ν-β is some function of thickness τ, so that at the line AC (fig. 6) the quantity ν-β is a constant (τ is constant) which fulfills the condition for a simple wave system upstream of the blades.

An exact and detailed analysis of the flow at the entrance region ABC was not included in the original scope of this report. The results of the flow computations to be presented are principally concerned with the flow downstream of characteristic AB; however, to determine the nature of the waves in the entrance region, rough calculations approximating the flow were made assuming the coefficients in the characteristic equations to be proportioned linearly along CB from the value at C to the value at B (fig. 6). At the blade leading edge, the inlet-flow direction was -67.4° and the suction-surface direction -66.4° so that there is a 1° expansion wave at the leading edge. A schematic sketch (fig. 6) shows the indications of the numerical results which are given in table I. The primed letters on figure 6 indicate points on the blade surface along corresponding characteristics. These results show that compressions as well as expansion are propagated upstream from AC even though expansion waves are generated from surface CB because of velocity changes along the characteristics. (These changes would be absent in plane flow.) The calculations further indicate little change in velocity and flow angle at the entrance to the blade passage so that assuming W and β constant along AC would have been a suitable assumption in this case.

If a detailed analysis of the entrance region flow is not required, the flow properties may be determined by a method similar to the one described in the following section for obtaining the first inlet characteristic line AB contained within the passage. The fact has been utilized that W sin β equal to a constant along a ξ-constant characteristic gives a simple wave system upstream of the blade row where τ is considered. Since it has been assumed that W sin β is constant, equations (23) and (24) show that T is also a constant.

Now with $W \sin \beta$ and T constant, the first expansion wave AB can be obtained by a simple graphical trial-and-error method. The relative velocity W^* is fixed and a trial value for β selected at A. By the procedure shown in appendix A, line AB is solved piecewise, that is, from A to D, D to E, and so forth, establishing W^* and β at each point. The value of β determined at B must agree with the value of the blade direction at B. The calculation is repeated from A to B until the value selected for β at A gives in the graphical solution the same β at B as given by the blade direction at that point. In this manner the inlet characteristic line (expansion wave) of figure 7 was obtained. The length of the segments AD, DE, and so forth establishes the size of the subsequent characteristic network since W^* and β are determined at these points for beginning the characteristic solution.

A Mach number of 1.6563 was prescribed at A in this example, fixing the relative velocity at 1.3308. An inlet angle of about -65° was desired; after the trial-and-error solution, an inlet angle of -67.4° at the leading edge was found to give the correct inlet expansion wave.

Characteristic solution blade-to-blade - The flow properties in the blade passage were determined using the finite difference form of characteristic equations (19) and (20) as shown in appendix B. The resultant characteristic network of approximately 100 grid points, where the flow properties were determined, is shown in figure 7.

The iterative procedure described earlier based upon averaged coefficients in the characteristic equations required from one to four iterations (usually two) to converge the relative velocity within one in the fourth decimal and the flow angle within one in the first decimal. The numerical setup used in the solution, together with a sample calculation, is shown in table IV.

Table II gives a comparison between the first and last iterations of the characteristic equations (19) and (20) for four of the grid points indicated in figure 7.

A calculation based upon continuity was carried out at the inlet and exit to determine what the magnitude of the relative velocity would be at the exit if the stream-filament-thickness reduction had not been taken into account as in a two-dimensional characteristic solution. It was found that the velocity W^* at the exit would be approximately 1.71 as compared with about 1.33 (see fig. 10) if the stream-filament-thickness effects were included. At each grid point the characteristic solution, compared with the plane-flow characteristics solution, indicated a reduction in relative velocity and absolute value of the flow angle when the stream-filament thickness was included in the characteristic equations.

Shock wave. - The presence of the blade in a supersonic stream produces a shock wave at the blade leading edge. In this example the shock wave is caused by the 7° deflection required of the flow in turning from the inlet angle of -67.4° to the pressure surface direction of -60.4° at the inlet.

Across the shock wave, the variation in the properties themselves no longer can be considered infinitesimal and continuous as required in the application of the characteristic equations; consequently, it is necessary to consider what happens when the shock wave crosses a characteristic line. Figure 8 illustrates a typical case where a shock wave from the leading edge intersects a characteristic line. The calculation of the flow properties for this situation is treated as follows: by ignoring the existence of the shock wave, an ordinary characteristic solution is carried out for point 3 (fig. 8). The intersection point between the shock wave and the ξ-characteristic line is then determined, and a linear interpolation is made between 2 and 3 for the flow properties at c. Knowledge of the flow properties ahead of the shock and the fact that the shock wave is a 7° compression wave permit the calculation of the flow behind the shock at point b from the general shock relations; the flow can also be determined from reference 7, as was done in this example. The values at b are used to continue the next characteristic point solution. Point 3 is needed only to interpolate for the values at c and no longer appears in the characteristic network.

It has been assumed in the calculations that the angle change (7°) is constant through the shock from the leading edge until it reaches the suction surface of the preceding blade. For a weak shock the flow deflection through the shock is independent of waves of the opposite family, so that a shock wave through a field of varying stream-filament thickness is also of constant deflection unless it is intersected by waves of the same family. As shown in figure 7, the leading-edge shock wave (heavy line) is not intersected by waves of the same family; therefore, the calculations assuming a constant deflection are computationally consistent. However, if a finer grid had been used, the shock would have coalesced with waves of the same family and an adjustment of the flow deflection would have been necessitated. This situation occurred with the reflection of the shock wave from the suction surface where it is shown in figure 7 to coalesce with expansion waves from the suction surface. The reflected shock wave was weakened from a 7° to a 2° deflection by the expansions from the suction surface.

Streamlines. - A stream function ψ which satisfies the continuity equation (I) may be defined as follows:

$$\frac{\partial \psi}{\partial \varphi} = r T \rho W \cos \beta \tag{25}$$

$$\frac{\partial \psi}{\partial z} = -\tau \rho W \sin \beta \tag{26}$$

The streamlines shown in figure 9 were determined by integrating the stream function (eqs. (25) and (26)) along a characteristic line extending across the blade passage. Thus,

$$\psi_3 - \psi = \int_{\varphi}^{\varphi_3} \left(\frac{\partial \psi}{\partial \varphi} + \frac{\partial \psi}{\partial z} \frac{1}{\lambda} \right) d\varphi = \int_{z}^{z_3} \left(\frac{\partial \psi}{\partial \varphi} \lambda + \frac{\partial \varphi}{\partial z} \right) dz \tag{27}$$

RESULTS AND DISCUSSION

For a subsonic-axial-velocity component at the inlet to the blade, the family of waves traveling upstream must be defined by a simple wave system in order to establish uniform-flow conditions at infinity. In this example the ξ-constant-characteristic family extends upstream, and a simple wave system in this region where τ is a constant is defined by ν-β equal to a constant. Also, if the curvature terms in the characteristic equations are neglected, W sin β equal to a constant along a ξ-constant characteristic approximates a simple wave system in the entrance region.

The characteristic solution shows a reduction in the absolute value of the flow angle and relative velocity in the blade passage from the two-dimensional characteristic solution when a stream-filament-thickness reduction from blade entrance to exit is considered in the characteristic equations. This result would be expected in supersonic flow since a flow-area reduction produces a decrease in velocity. The flow properties obtained from the last iteration using equations (19) and (20) and the first iteration calculation check well, indicating that one iteration calculation may be sufficient. It is estimated that a solution neglecting stream-filament curvature terms obtained with equations (19) and (20), which is facilitated by using the Ames tables (ref. 6), would require 1/2 hour of experienced computing time to converge a characteristic point.

The streamlines determined are presented in figure 9. As would be expected for supersonic flow, the streamline spacing increases from pressure to suction surface. On the pressure surface are given the maximum ψ-values divided by ψ-maximum at the inlet; these values are determined by integrating along ξ-constant-characteristic lines. These values show that continuity in the passage checked within ± 2 percent.

Figure 10 shows the velocity distribution obtained on the blade surfaces. The abrupt decrease in velocity on the suction surface at $z \approx 0.25$ is caused by the impingement of the leading edge shock wave on the suction surface at this point. The shock wave, noticeably decreased in strength, is reflected to the pressure surface at $z \approx 0.505$ where a lesser decrease in relative surface velocity occurs. The arithmetical mean velocity shown by the dashed line is approximately the same at inlet and exit, an indication that the area normal to the flow is the same at entrance and exit.

The local static to relative upstream total pressure ratio on the blade surfaces is shown in figure 11. The sharp rise in pressure at $z \approx 0.25$ and $z \approx 0.505$ is caused by the shock wave. The average pressure shown by the dashed line gives an indication of the type of pressure distribution that may be expected from pressure measurements at the impeller outer wall.

No simplified method of correcting for the stream-filament thickness could be found due to the interdependence of β and W in the characteristic equations. The thickness correction as it is used here is applicable to thin sheets, since the thickness effect is actually propagated along characteristic lines in the meridional plane. The result is a translation downstream of the thickness effect from the axial station where the thickness actually existed. For thin sheets the translation is negligible. It may be desirable to reiterate the solution with a new stream-filament-thickness distribution based upon the most recent velocity distribution. For the solutions suggested here to determine τ^*, other fluid effects such as vorticity and secondary flows will cause the actual flow to deviate from the hypothetical flow; hence, any gain by further refinements in τ^* may be masked by the other fluid properties which have been neglected in the solution.

CONCLUDING REMARKS

The method of characteristics has been used to solve the supersonic flow equations; this method gives the blade-to-blade flow properties along an arbitrary stream surface of revolution where the meridional thickness associated with the surface of revolution is determined by an axisymmetric solution.

The results indicate an appreciable difference between the flow properties calculated with the two-dimensional characteristic equations, considering ordinary two-dimensional flow, and those determined with the characteristics method demonstrated here. For this particular example the effect of the stream-filament reduction between the blade-passage entrance and exit was to reduce the relative velocity and the absolute value of the flow angle. In the entrance region it is shown that

expansion waves propagated along characteristics become compression waves because of the stream-filament-thickness variation. This effect of the stream filament will result in an inlet-angle change upstream from that determined for two-dimensional flow.

Expressing the characteristic equations in terms of the Prandtl-Meyer variable ν enables the Ames tables to be utilized in the computation procedure. The solution indicates that first iteration calculations gave flow properties of sufficient accuracy. Each grid point takes approximately 1/2 hour to calculate, depending upon the number of iterations required.

Lewis Flight Propulsion Laboratory
National Advisory Committee for Aeronautics
Cleveland, Chio, April 17, 1953

APPENDIX A

INLET CHARACTERISTIC CALCULATION

The following conditions were prescribed at the leading edge point, 5,0 (fig. 7), for the calculation of the inlet characteristic:

$$M_{5,0} = 1.6563$$

$$W^*_{5,0} = 1.3308$$

$$\tau^*_{5,0} = 0.05$$

$$\beta_{5,0} = -67.4^\circ$$

where $z^*_{5,0} = 0.00$, $r^*_{5,0} = 1.0$, and $\varphi_{5,0} = 0.2167$. The value for $\beta_{5,0}$ was found to give the correct β at the characteristic-line intersection, 0,0, on the suction surface after a series of solutions similar to that shown below. Along this inlet characteristic,

$$T^* = \text{constant} = (\tau^* \rho^* W^* \cos \beta)_{5,0} = 0.008568$$

where $\rho^* = \frac{\rho}{\rho_a}$, and

$$(W^* \sin \beta)_{5,0} = \text{constant} = -1.2286$$

With T^*/τ^* and $(W^* \sin \beta)^2$ as parameters, a straight-line equation can be developed from which the inlet characteristic curve, and flow properties may be determined. Let

$$T^*/\tau^* = d = \rho^* W^* \cos \beta \tag{A1}$$

and upon substitution of

$$\rho^* W^* = 0.578688 \frac{A^*_{cr}}{A^*}$$

into equation (A1), it becomes

$$d = \left(0.578688 \frac{A^*_{cr}}{A^*}\right) \cos \beta \tag{A2}$$

If

$$e = W^* \sin \beta \tag{A3}$$

the substitution of equations (A2) and (A3) into

$$1 = \cos^2\beta + \sin^2\beta$$

results in the following relation:

$$\frac{1}{\left(0.578688 \frac{A^*_{cr}}{A^*}\right)^2} = \frac{1}{d^2} - \frac{e^2/d^2}{W^{*2}} \tag{A4}$$

Equation (A4) is the equation for a straight line as shown in figure 12 with an ordinate intercept equal to $1/d^2$ and a negative slope of e^2/d^2. Another relation between $\frac{1}{\left(0.578688 \frac{A^*_{cr}}{A^*}\right)^2}$ and W^{*2} can be determined from the energy relation. This relation is

$$\frac{1}{\left(0.578688 \frac{A^*_{cr}}{A^*}\right)^2} = \frac{1}{W^{*2}} \left(1 - \frac{\gamma-1}{2} W^{*2}\right)^{\frac{2}{1-\gamma}} \tag{A5}$$

The nature of equation (A5) is also shown in figure 12. The intersection of the curve representing equation (A5) with the straight line gives the value of the relative velocity. Straight lines in agreement with the inlet boundary conditions are calculated for a series of selected grid points. Once the velocity is determined from a plot similar to figure 12, the flow angle can be calculated from equation (A3).

The final inlet characteristic calculation is shown in table III. Grid points were selected at approximately five equal intervals as shown in figure 7.

APPENDIX B

CHARACTERISTIC CALCULATION IN BLADE PASSAGE

Characteristic Equations (19) and (20)

The variables ν and β in characteristic equations (19) and (20) can be expressed as a two-dimensional ν and β plus a correction term. Let

$$\nu = \nu_o + \epsilon \tag{B1}$$

$$\beta = \beta_o + \delta \tag{B2}$$

Then equations (19) and (20) may be written as:

$$d(\nu_o+\epsilon) - d(\beta_o+\delta) + G\, d(\ln \tau^*) = 0 \quad (\eta \text{ constant}) \tag{B3}$$

$$d(\nu_o+\epsilon) + d(\beta_o+\delta) - F\, d(\ln \tau^*) = 0 \quad (\xi \text{ constant}) \tag{B4}$$

where F and G are the coefficients of the thickness term in equations (19) and (20). Since for the two-dimensional characteristics

$$d\nu_o - d\beta_o = 0 \quad (\eta \text{ constant})$$

$$d\nu_o + d\beta_o = 0 \quad (\xi \text{ constant})$$

equations (B3) and (B4) when integrated along the characteristic curve become:

$$\epsilon_3 - \delta_3 + \int_1^3 G\, d(\ln \tau^*) = 0 \quad (\eta \text{ constant}) \tag{B5}$$

$$\epsilon_3 + \delta_3 - \int_2^3 F\, d(\ln \tau^*) = 0 \quad (\xi \text{ constant}) \tag{B6}$$

For trapezoidal integration between characteristic points 1 and 3 and points 2 and 3 and for averaged coefficients F and G, the resulting correction terms are:

$$\epsilon_3 = \frac{F(\ln \tau_3^* - \ln \tau_2^*) - G(\ln \tau_3^* - \ln \tau_1^*)}{2} \tag{B7}$$

$$\delta_3 = \frac{F(\ln \tau_3^* - \ln \tau_2^*) + G(\ln \tau_3^* - \ln \tau_1^*)}{2} \tag{B8}$$

When the two-dimensional solution calculated in equations (B9) to (B12) is utilized, ϵ_3 and δ_3 at point 4,3 can be calculated as shown in table IV. This procedure is representative of the type of solution required for characteristic equations (19) and (20).

Plane-Flow Characteristic Equations (21) and (22)

$$(\nu_1 - \nu_3) - (\beta_1 - \beta_3) = 0 \quad (\eta \text{ constant}) \tag{B9}$$

$$(\nu_2 - \nu_3) + (\beta_2 - \beta_3) = 0 \quad (\xi \text{ constant}) \tag{B10}$$

Solving for ν_3 and β_3,

$$\nu_3 = \frac{(\nu_1 + \nu_2) + (\beta_2 - \beta_1)}{2} \tag{B11}$$

$$\beta_3 = \frac{(\beta_1 + \beta_2) - (\nu_1 - \nu_2)}{2} \tag{B12}$$

Calculations at grid point 4,3 are shown in table V.

REFERENCES

1. Wu, Chung-Hua: A General Theory of Three-Dimensional Flow in Subsonic and Supersonic Turbomachines of Axial-, Radial-, and Mixed-Flow Types. NACA TN 2604, 1952.

2. Goldstein, Arthur W.: Axisymmetric Supersonic Flow in Rotating Impellers. NACA Rep. 1083, 1952. (Supersedes NACA TN 2388.)

3. Wu, Chung-Hua, and Costilow, Eleanor L.: A Method of Solving the Direct and Inverse Problem of Supersonic Flow along Arbitrary Stream Filaments of Revolution in Turbomachines. NACA TN 2492, 1951.

4. Brand, Louis: Vector and Tensor Analysis. John Wiley & Sons, Inc., 1948.

5. Courant, R., and Friedrichs, K. O.: Supersonic Flow and Shock Waves. Interscience Pub., Inc., 1948.

6. The Staff of the Ames 1- by 3-Foot Supersonic Wind-Tunnel Section: Notes and Tables for Use in the Analysis of Supersonic Flow. NACA TN 1428, 1947.

7. Neice, Mary M.: Tables and Charts of Flow Parameters Across Oblique Shocks. NACA TN 1673, 1948.

TABLE I. - APPROXIMATE ENTRANCE REGION FLOW PROPERTIES

[a]Point	Relative flow angle, β, deg	Relative velocity, W^*	[a]Point	Relative flow angle, β', deg	Relative velocity, $W^{*\prime}$
C	-66.4	1.347	C'	-66.4	1.347
S	-67.0	1.337	S'	-66.0	
R	-67.3	1.331	R'	-65.4	to
Q	-66.9	1.337	Q'	-64.0	
A	-67.4	1.331	B	-63.4	1.374

[a]Points defined on fig. 6.

TABLE II. - COMPARISON OF CHARACTERISTIC SOLUTIONS AT FOUR GRID POINTS

Grid point	Grid property	Characteristic equations (19) and (20), first iteration	Characteristic equations (19) and (20), n^{th} iteration
2,1	β	-59.82°	-59.72°
	W^*	1.4124	1.4150
3,1	β	-60.60°	-60.54°
	W^*	-1.4009	1.4033
4,3	β	-46.56°	-46.61°
	W^*	1.5539	1.5527
9,4	β	-11.66°	-11.65°
	W^*	1.3864	1.3869

TABLE III. - INLET CHARACTERISTIC CALCULATION

	①	②	③	④	⑤	⑥	⑦
Grid point	z^*, arbitrarily selected along inlet line, AB	τ^*, figure 4 and ①	d, $\frac{0.008568}{②}$	$\frac{1}{d^2}$, $\frac{1}{③^2}$	$\frac{e^2}{d^2}$, 1.509 × ④	$\frac{1}{W^{*2}}$, assume arbitrarily to find straight line	Straight line points, ④ - ⑤ ⑥
4,0	0.0085	0.04875	0.17575	32.3749	48.8699	0.575 .550	4.2747 5.4965
3,0	0.0155	0.04777	0.17936	31.0849	46.9227	0.575 .550	4.1043 5.2774
2,0	0.0220	0.04690	0.18269	29.9620	45.2276	0.525 .550	6.2175 5.0868
1,0	0.0270	0.04618	0.18553	29.0516	43.8534	0.525 .555	6.0286 4.9322
0,0	0.0318	0.04555	0.18810	28.2632	42.6633	0.525 .550	5.8650 4.7984

	⑧	⑨	⑩	⑪	⑫	⑬	⑭
Grid point	$\frac{1}{W^{*2}}$, intersection fig. 12	W^*, $\sqrt{\frac{1}{⑧}}$	sin β, $\frac{-1.2286}{⑨}$	β, $\sin^{-1}$ ⑩, deg	M, ref. 6	μ, $\sin^{-1}\frac{1}{⑫}$, deg	λ_-, ⑪ - ⑬, deg
5,0		1.3308		-67.400	1.6563		
4,0	0.5571	1.3398	-0.91700	-66.492	1.6731	36.705	-103.197
3,0	0.5501	1.3483	-0.91122	-65.675	1.6901	36.276	-101.951
2,0	0.5432	1.3568	-0.90551	-64.892	1.7070	35.861	-100.753
1,0	0.5361	1.3658	-0.89955	-64.099	1.7251	35.428	-99.527
0,0	0.5297	1.3740	-0.89418	-63.411	1.7418	35.038	-98.449

TABLE IV. - CHARACTERISTIC CALCULATION EQUATIONS (19) AND (20)

Grid point	Grid point	①	②	③	④	⑤	⑥
	1	β	μ			④×③	④ - ③
		β_1	μ_1	cot ①$_1$	tan ②$_1$		
3	2	β_2	μ_2	cot ①$_2$	tan ②$_2$		④ + ③
4,3	4,2	-56.00	31.77	-0.67450	0.61930	-0.41772	1.29280
	0,3	-45.98	27.04	-.96636	.51040	-.49323	-.45596

Grid point 3	⑦	⑧	⑨	⑩	⑪	⑫
	G, F, ⑤/⑥	Table V column values		⑧×⑨	(⑨-⑧)/(⑨+⑧)	G_o, F_o, ⑩/⑪
		cot [4]	tan [8]			
4,3	-0.32311	-0.93546	0.49988	-0.46762	1.43534	-0.32579
	1.08174				-.43558	1.07356

Grid point 3	⑬	⑭	⑮	⑯	⑰	⑱
	G, F, Average, (⑦+⑫)/2	z_3	τ_3^*	τ_1^*	ln ⑮	ln ⑯
				τ_2^*		
4,3	-0.32445	0.1368	0.03430	0.03877	-3.37260	-3.25010
	1.07765			.03519		-3.34698

Grid point 3	⑲	⑳	㉑	㉒	㉓	㉔
	⑰ - ⑱	⑬ × ⑲	ϵ_3, (⑳$_2$ - ⑳$_1$)/2 X57.2958, deg	δ_3, (⑳$_2$ + ⑳$_1$)/2 X57.2958, deg	Table V column values	
					ν_o, [3]	β_o, [4]
4,3	-0.12250	0.03974	-1.93	0.35	32.66	-46.91
	-.02562	-.02761				

Grid point 3	㉕	㉖	㉗	㉘	㉙	㉚	㉛	㉜
	ν_3, ㉓ + ㉑, deg	β_3, ㉔ + ㉒, deg	M, ㉕ and ref. 6	$\frac{a}{a_a}$, ㉕ and ref. 6	W_3^*, ㉗ × ㉘	μ_3, ㉕ and ref. 6, deg	λ_{+3}, ㉖ + ㉚, deg	λ_{-3}, ㉖ - ㉚, deg
4,3	30.73	-46.56	2.1615	0.7185	1.5539	27.02	-19.54	-73.58

TABLE V. - PLANE-FLOW CHARACTERISTIC CALCULATION

EQUATIONS (21) AND (22)

		①	②	③	④
Grid point 3	Grid points 1	ν_1	β_1	ν_3, $[①_1 + ①_2 + ②_2 - ②_1] \div 2$	β_3, $[②_1 + ②_2 - ①_1 + ①_2] \div 2$
	2	ν_2	β_2		
4,3	4,2	23.57	-56.00	32.66	-46.91
	0,3	31.73	-45.98		

	⑤	⑥	⑦	⑧	⑨	⑩
Grid point 3	M, ③ and ref. 6	a/a_a, ③ and ref. 6	W_3^*, ⑤×⑥	μ_3, ③ and ref. 6	λ_{+3}, ②+⑧, deg	λ_{-3}, ②-⑧, deg
4,3	2.236	0.7071	1.5811	26.56	-20.35	-73.47

NACA

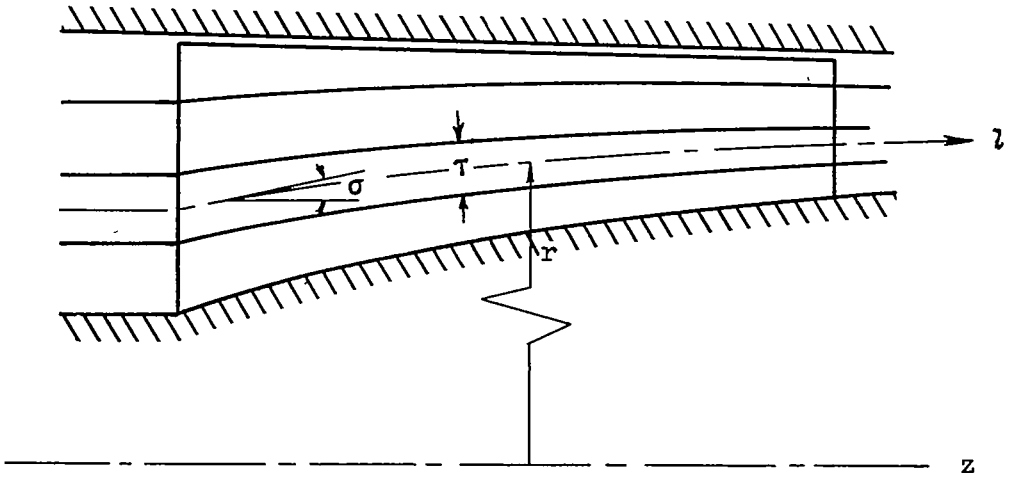

Figure 1. - General stream filament of revolution.

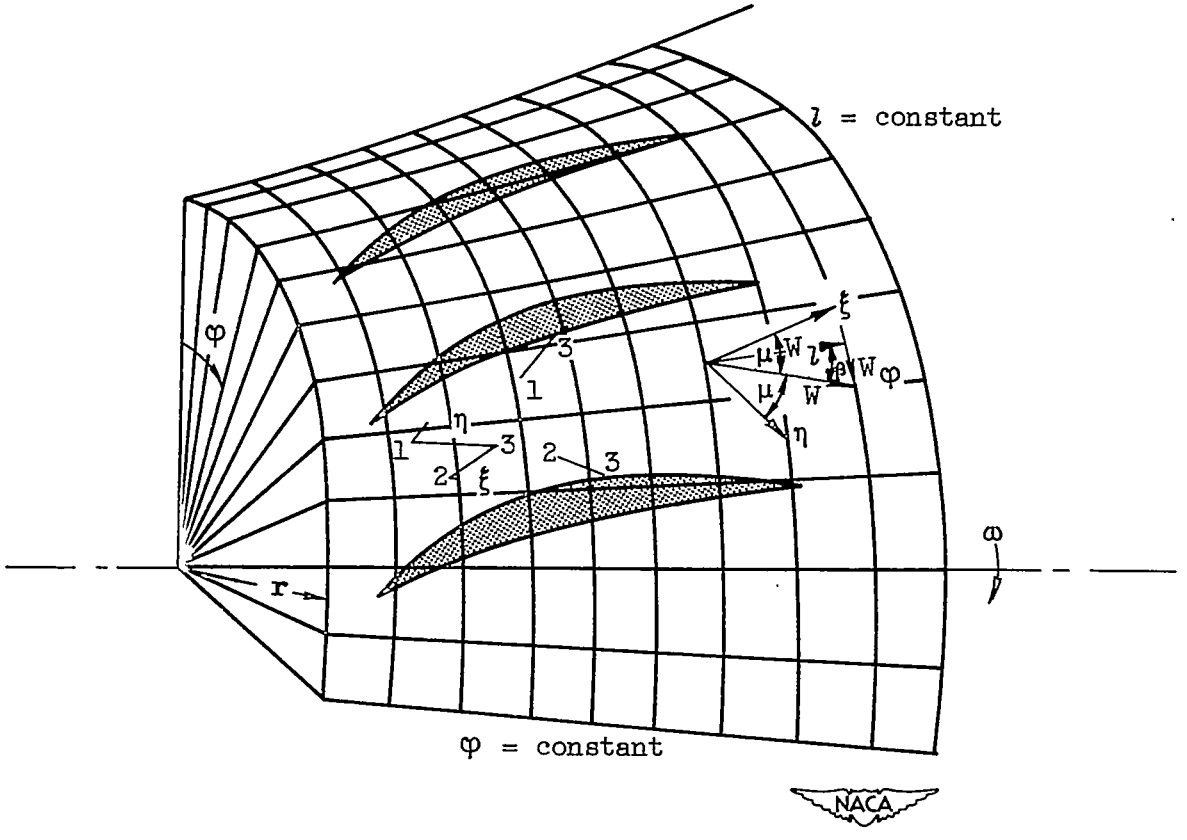

Figure 2. - Blade section and characteristic calculating points on mean surface of revolution.

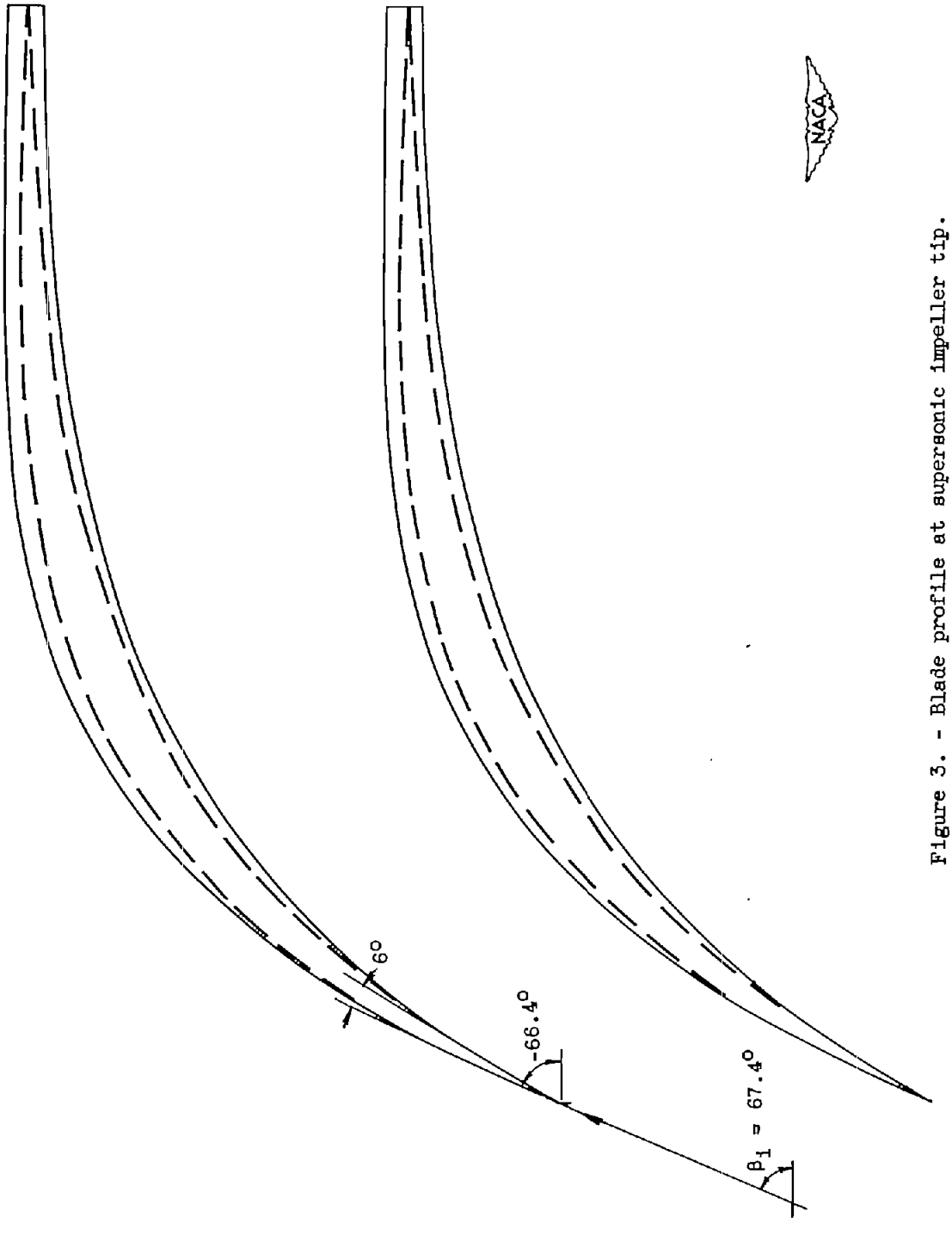

Figure 3. - Blade profile at supersonic impeller tip.

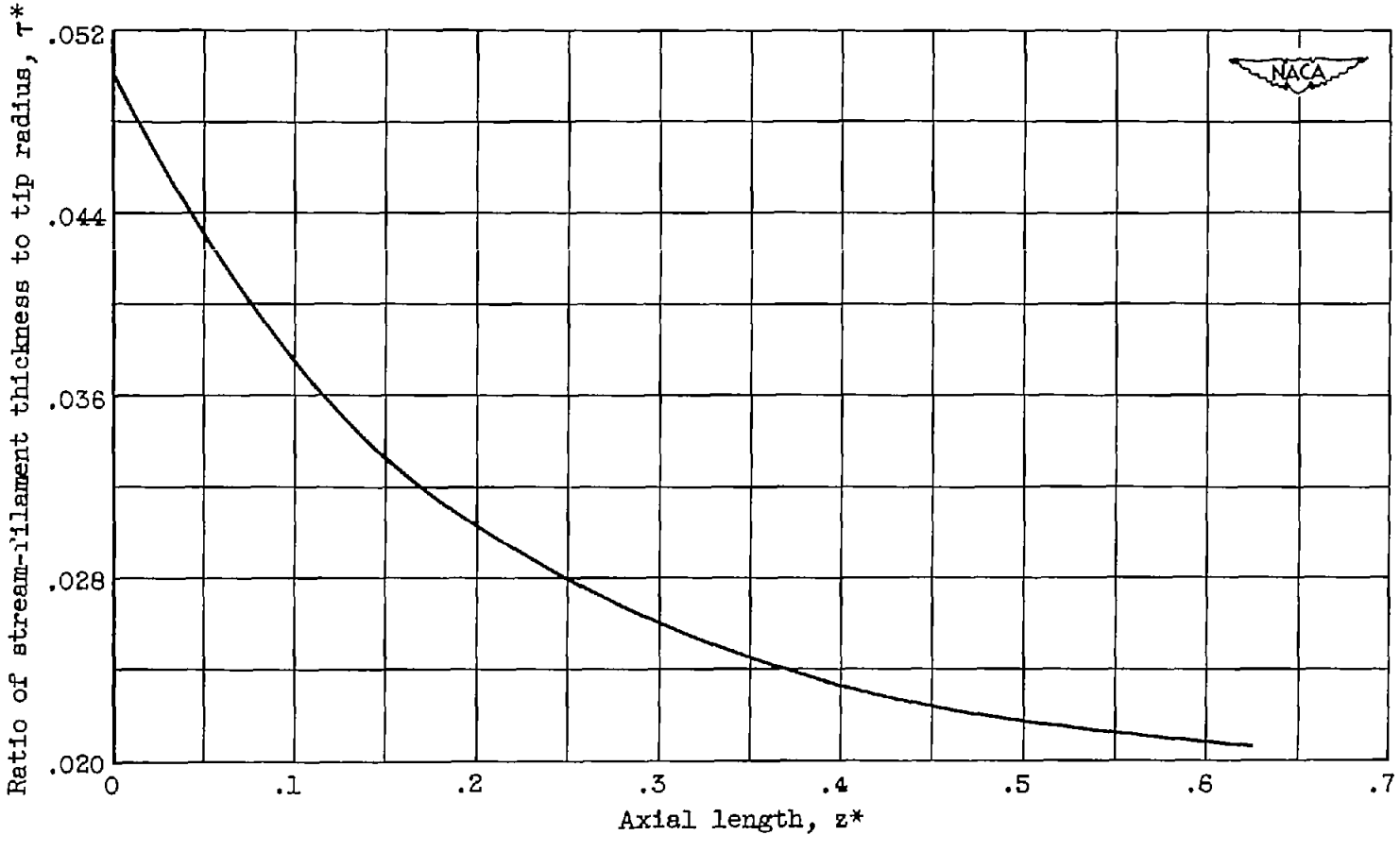

Figure 4. - Variation of stream-filament thickness with axial length.

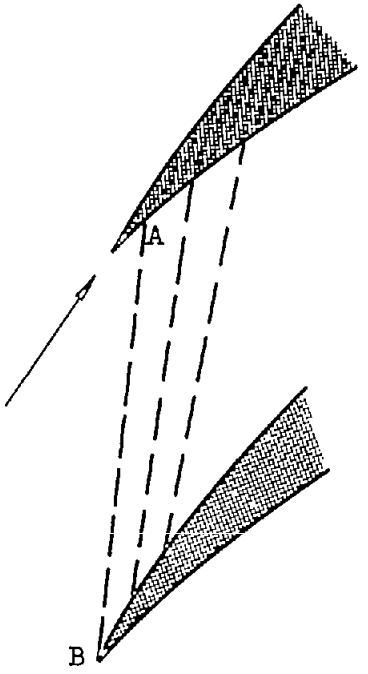

Figure 5. - Expansion waves contained in blade passage entrance section.

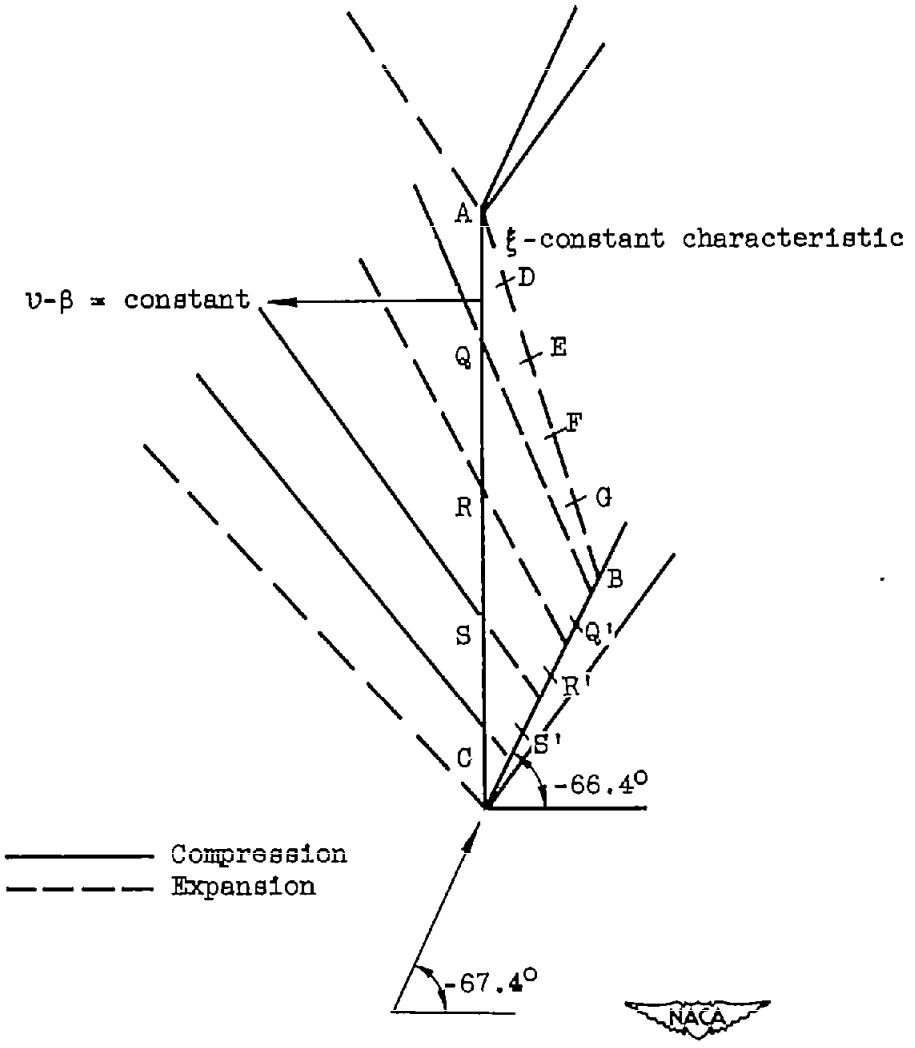

Figure 6. - Wave system extending upstream in blade passage entrance section.

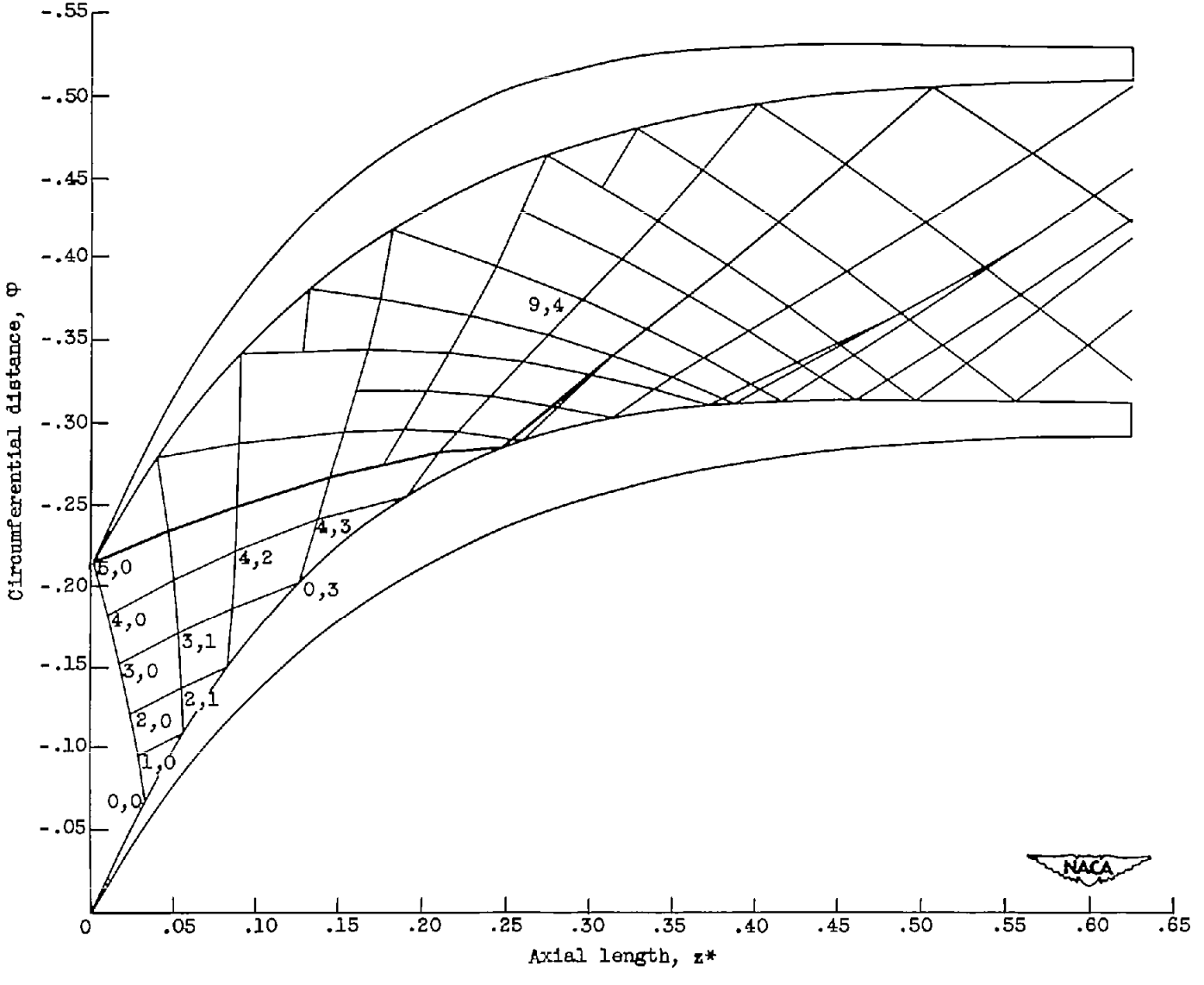

Figure 7. - Characteristic network at supersonic impeller tip.

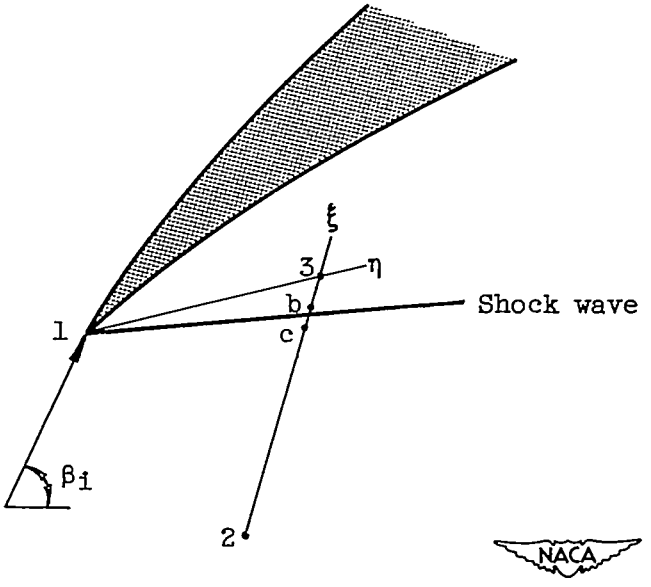

Figure 8. - Shock-wave intersection with characteristic line.

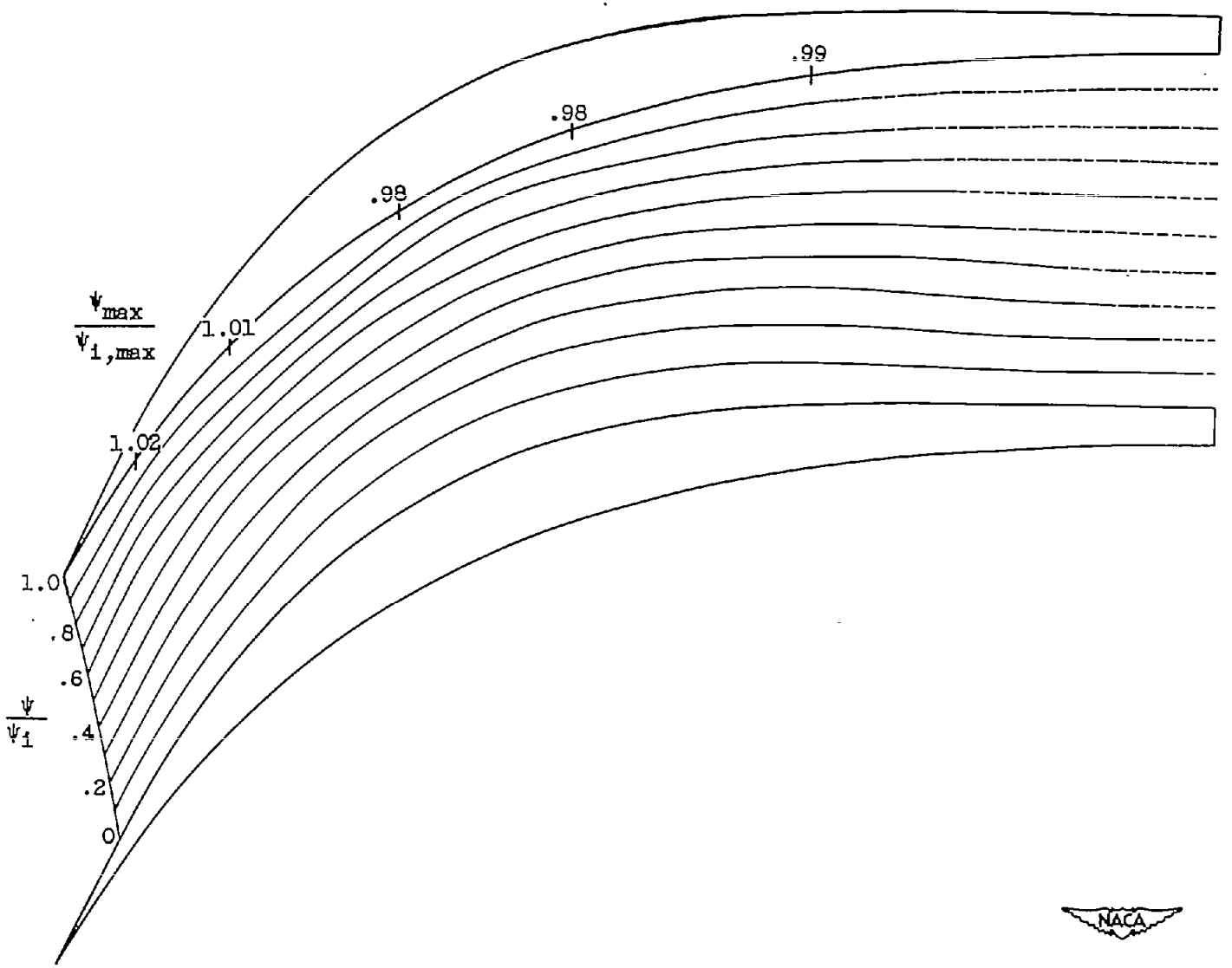

Figure 9. - Streamlines in blade passage at supersonic impeller tip.

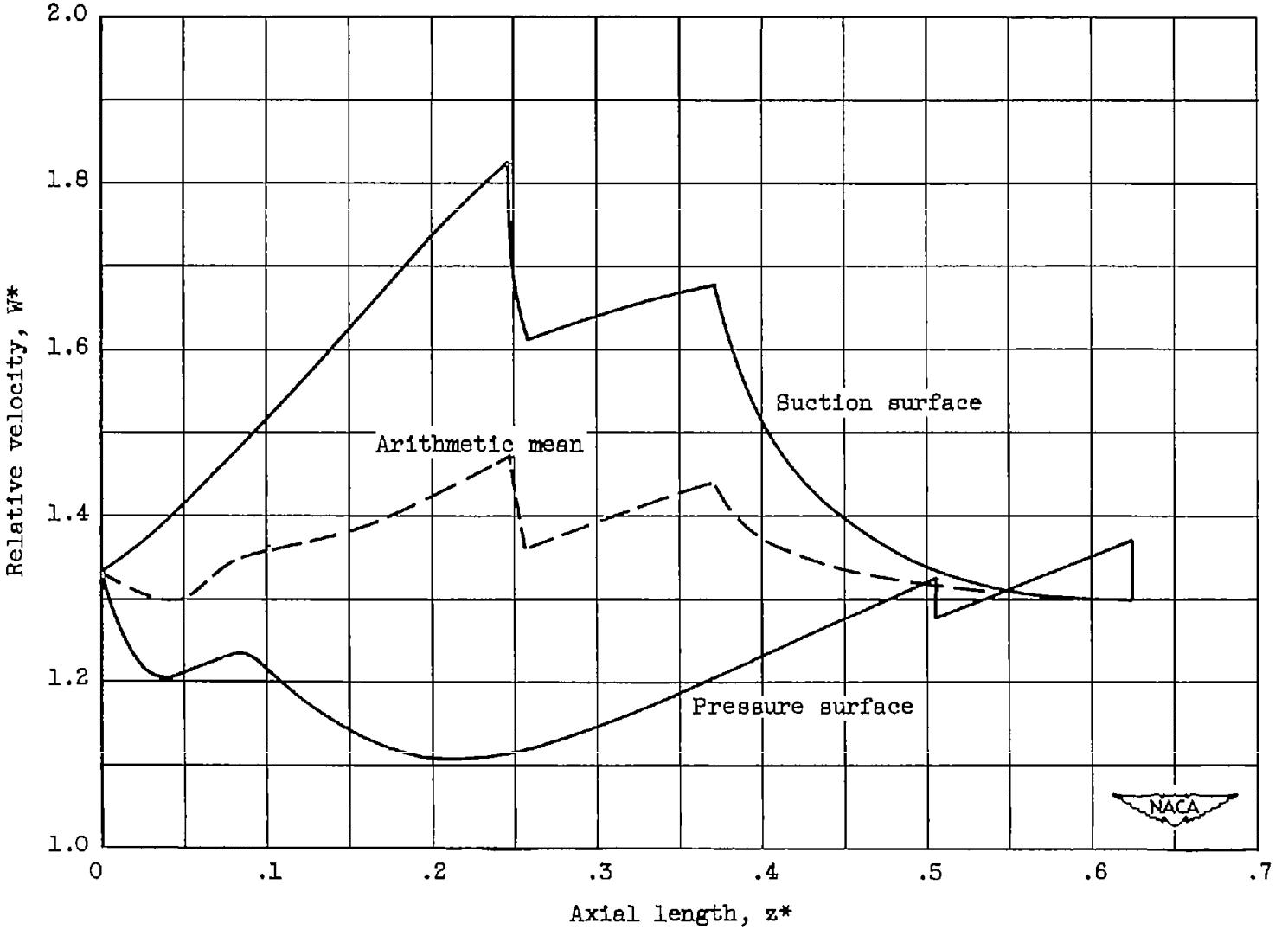

Figure 10. - Velocity distribution on blade surfaces at supersonic impeller tip.

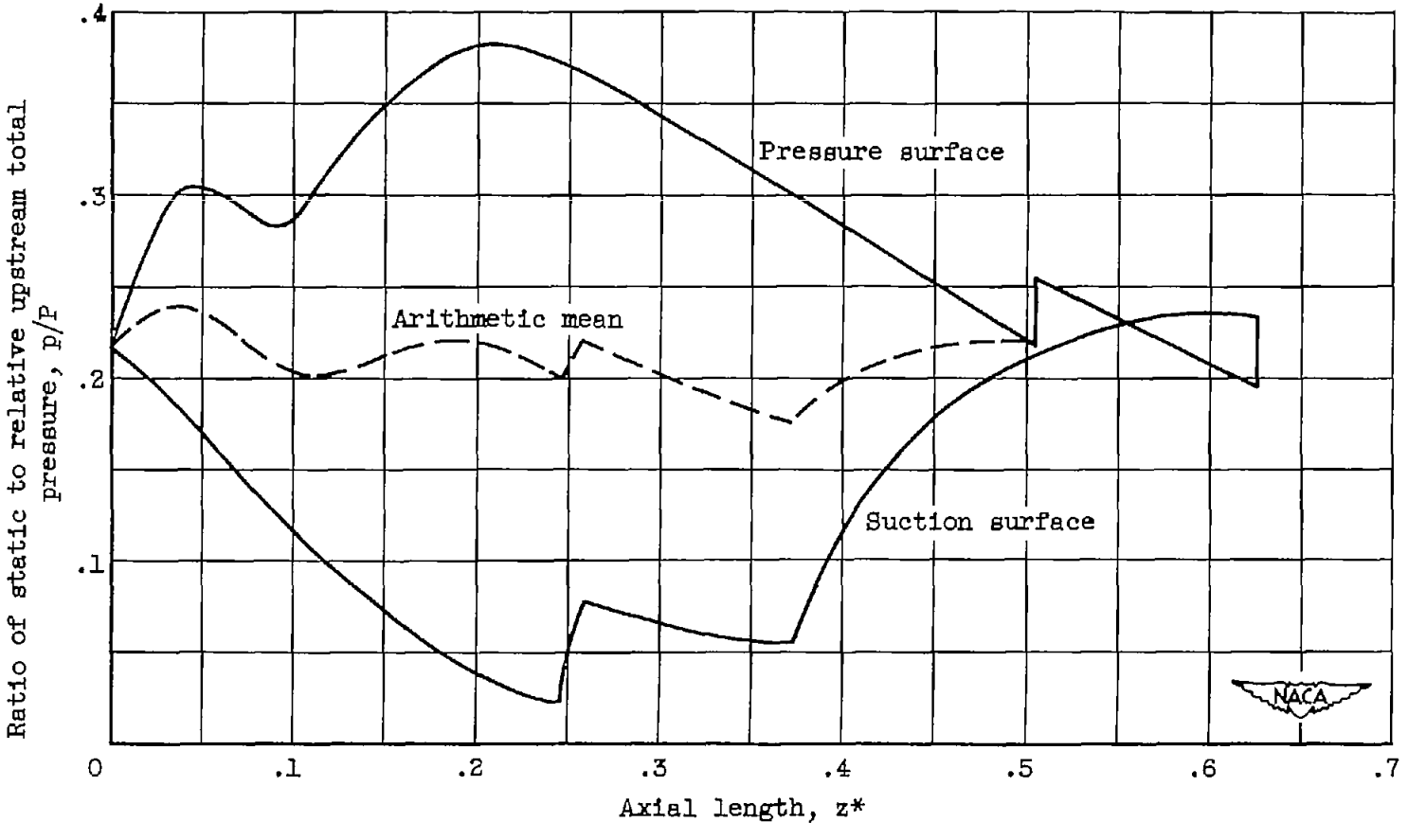

Figure 11. - Static-pressure distribution on blade surfaces at supersonic impeller tip.

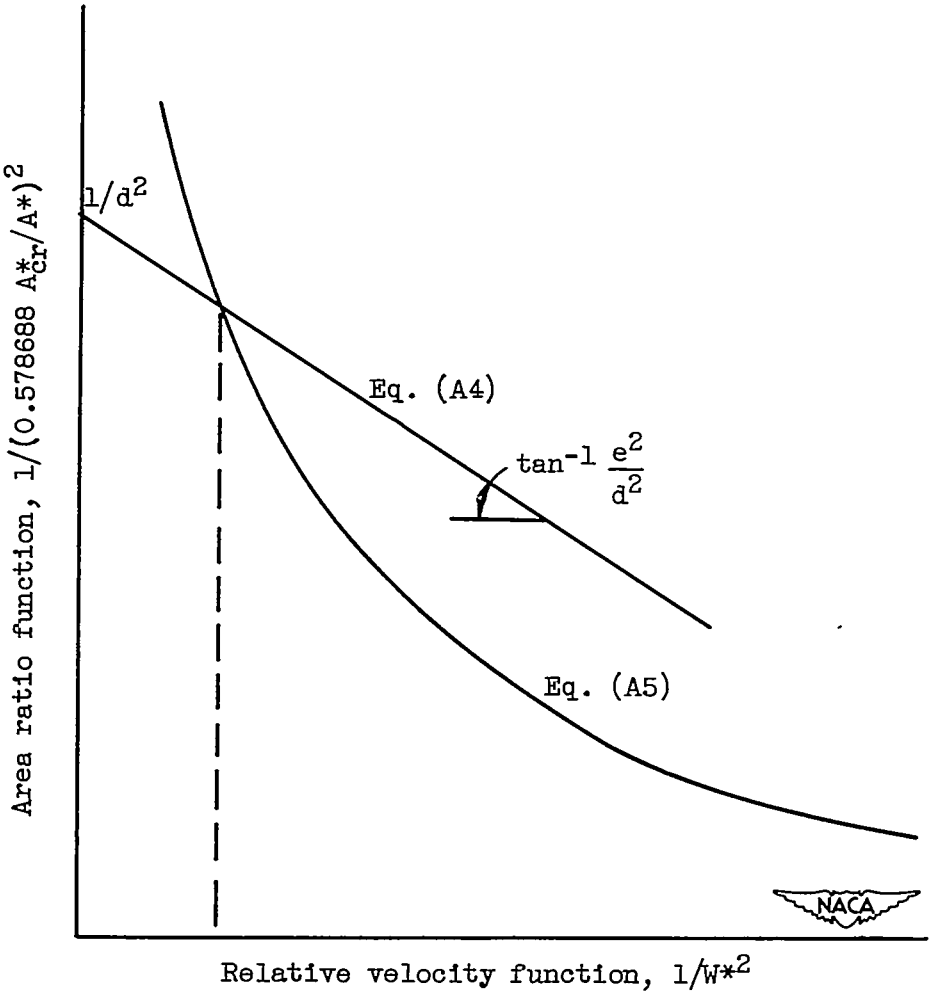

Figure 12. - Relative velocity as function of area ratio for relative velocity determination along inlet line.

NACA-Langley - 8-7-53 - 1000